

# Assembly Tests of the First Nb<sub>3</sub>Sn Low-beta Quadrupole Short Model for the Hi-Lumi LHC

H. Pan, D. W. Cheng, E. Anderssen, G. Ambrosio, H. Felice, J. C. Perez, M. Juchno, P. Ferracin, S.O.Prestemon,

**Abstract**— In preparation for the high luminosity upgrade of the Large Hadron Collider, the LHC Accelerator Research Program (LARP) in collaboration with CERN is pursuing the development of MQXF: a 150 mm aperture high-field Nb<sub>3</sub>Sn quadrupole magnet. The development phase starts with the fabrication and test of several short models (1.2 m magnetic length) and will continue with the development of several long prototypes. All of them are mechanically supported using a shell-based support structure, which has been extensively demonstrated on several R&D models within LARP. The first short model MQXFS-AT has been assembled at LBNL with coils fabricated by LARP and CERN. In this paper, we summarize the assembly process and show how it relies strongly on experience acquired during the LARP 120 mm aperture HQ magnet series. We present comparison between strain gauges data and finite element model analysis. Finally we present the implication of the MQXFS-AT experience on the design of the long prototype support structure.

**Index Terms**—High Luminosity LHC (HL-LHC), Interaction Regions, quadrupole, LARP, Nb<sub>3</sub>Sn magnet, shell-based support structure, short model.

## I. INTRODUCTION

THE LARGE HADRON COLLIDER is preparing for the High Luminosity Upgrade. Key components of this upgrade are the Interaction region Low- $\beta$  Quadrupoles Q1, Q2 and Q3 [1]. The 150 mm aperture Nb<sub>3</sub>Sn magnets are developed in collaboration between the US-LARP (LHC Accelerator Research Program) and CERN. In this framework, the US is in charge of the ten Q1 and Q3 cold masses; each of them being made out of two 4.9 m long magnets called MQXFA. Each MQXFA magnet has a magnetic length of 4.2 m at cold and is assembled in a stand-alone support structure [2].

The development of these magnets follows a two-step process with the fabrication, assembly and test of the short (MQXFS) and the long prototypes (MQXFA). The MQXFS prototypes are built in collaboration between CERN and LARP, whereas the long prototypes are under the US responsibility. In the past months, mechanical models of the short magnets using aluminum false coils have been assembled and cooled down to validate the support structure both at CERN and within LARP. Results showing excellent agreement between strain gauges data and analysis are

Manuscript received October 20, 2015. This work was supported by the, U.S. Department of Energy, Office of Science under contract No. DE-AC02-05CH11231 and under Cooperative Agreement DE-SC0000661.

H.Pan (email: [hengpan@lbl.gov](mailto:hengpan@lbl.gov)), H. Felice, D.W.Cheng, S.O.Prestemon, E. Anderssen are with the Lawrence Berkeley National Laboratory, Berkeley, CA 94720 USA.

P. Ferracin, M. Juchno and J.C. Perez are with CERN, 1211 Geneva, Switzerland.

G. Ambrosio is with FNAL, Batavia, IL 60510 USA.

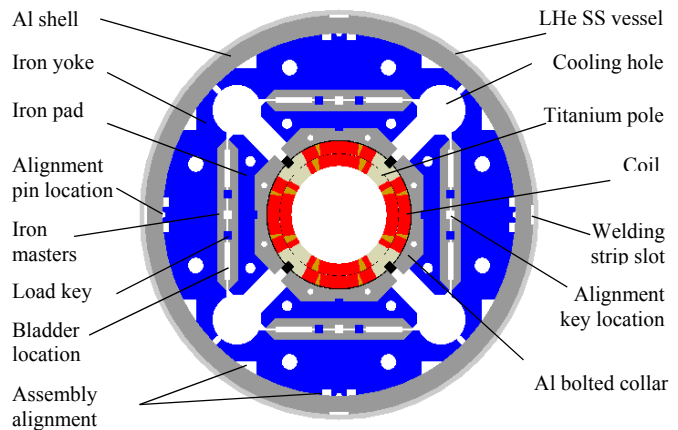


Fig. 1. Cross section of the MQXFS1 magnet.

reported in [3]. Here, we focus on the first mechanical assembly of the magnet using four real coils and we show how the assembly process is a direct application of the experience gained with LQ and HQ [4]. The experience gained will then guide the long structure scale-up to MQXFA.

## II. SHELL-BASED SUPPORT STRUCTURE IN MQXFS

### A. Magnet cross-section

The support structure used in the MQXF short and long prototypes is a shell-based support structure with the “bladder and key” concept, developed at LBNL for strain sensitive material such as Nb<sub>3</sub>Sn [5]. The “bladder and key” concept relies on partial preloading at room temperature and on the differential thermal contraction between the aluminum shell and the iron yokes during cool-down. This concept allows reversible assembly process and tunable preload, which has been extensively used and demonstrated within LARP. From the first prototype quadrupoles TQ [6] to the most recent LARP model HQ [7], the support structure has evolved to provide alignment features in addition to the tunable preload capability.

TABLE I  
MQXFS COIL AND MAGNET PARAMETERS

Parameter	Units	
Structure length with splice box	mm	2158
Magnet (LHe vessel) outer diameter	mm	630
Coil clear Aperture diameter	mm	150
No. turns in layer 1/2 (octant)		22/28
Nominal gradient $G_{nom}$	T/m	132.6
Nominal current $I_{nom}$	kA	16.47
Nominal conductor peak field $B_{nom}$	T	12.1
Stored energy density in straight sect. at $I_{nom}$	MJ/m	1.17
Differential inductance at $I_{nom}$	mH/m	8.21
$F_x/F_y$ (per octant) at $I_{nom}$	MN/m	+2.47/-3.48
$F_z$ (entire magnet) at $I_{nom}$	MN	1.17

The MQXF support structure is a scale-up from the HQ magnets [8]. As shown in Fig. 1, the coil-collar subassembly include four aluminum collars bolted around the coils, engaging the G11 pole alignment key, providing alignment between the coils and the support structure. This collar-pack is surrounded by four pads, made of magnetic steel in the straight section area of the magnet and of stainless steel at the extremities, which minimizes the field in the magnet ends. The pads are aligned with the collars via a slot and key feature at the mid-plane. This assembly forms the coil-pack subassembly, which is inserted into the yoke shell-subassembly. The pads are aligned with the yoke quadrants by an alignment key between both magnetic steel master key halves.

### B. Magnet integration features

As described in [9], the short prototype includes preliminary integration features such as cut-outs in the shell for both tack welding the LHe vessel and for accessing the yoke alignment features during assembly processes (Fig.2). These shell cut-outs have been optimized for uniform coil preload distribution, but remain under discussion toward the long prototype MQXFA.

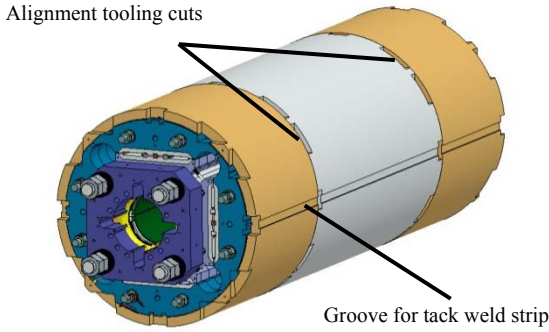


Fig. 2. Integration features of the short model.

## III. MAGNET ASSEMBLY

### A. Coil pack assembly

Ensuring proper preload of the coils is paramount for the magnet performance. The previous experience in LARP has shown the importance of properly matching the collar inner diameter with the coil outer diameter [10, 11], where improper matching of the radial surfaces may cause either bending (tension) of the pole piece and ineffective preload, or non-uniform loading on the pole turns. Matching is achieved by taking CMM (Coordinate Measuring Machine) data of the impregnated coils and iteratively shimming the radius to match the inner radius of the collars. These radial shims are made up of G10 and Kapton® sheets in various thicknesses. As this is an iterative process, pressure-sensitive film is used in the early stages of this process as a visual confirmation of a good match. To even out the contact pressure on coils, a slightly oversized collar radius is typically preferred to ensure support on the mid-plane.

Of the four coils assembled in the MQXFS Assembly Test

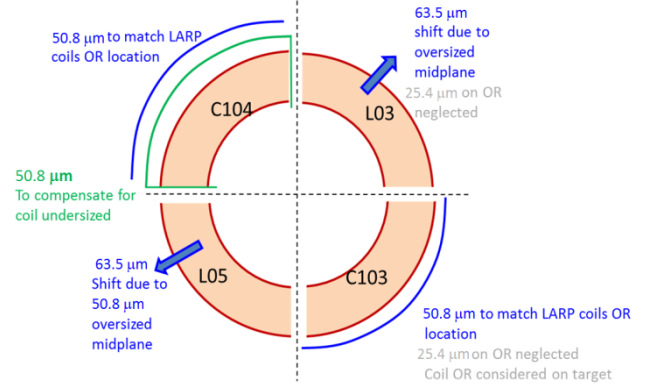


Fig. 3. Radial shimming plan of the given coil sizes (dimensions in inches).

(MQXFS-AT), two coils each were fabricated by CERN (coils 103 and 104) and LARP (coils 3 and 5). The CMM data of the coils' outer diameter and mid-planes show differences between the coils: the CERN coils measured consistently smaller than the nominal coil radius by about 50  $\mu\text{m}$  or more, whereas the LARP coils measured consistently larger by about 50  $\mu\text{m}$  on the outer radius.

To correct the size deviation among the four coils, and to ensure that all the coils' inner turns are located on a similar radius, additional shimming on the CERN coils was applied (Fig. 3): 50  $\mu\text{m}$  Kapton® was added on the outer diameter (OD) of coil 103; for coil 104, 100  $\mu\text{m}$  Kapton® was applied on the OD, and an additional 50  $\mu\text{m}$  was added to the mid-plane.

The MQXFS magnet underwent five collar-pack assembly iterations: three of them with different radial shimming, and two tests with different alignment key shims. Pressure sensitive films have been used in the assembly iteration (shown in Table II) to check the contact pressures on the collar-coil interfaces.

TABLE II  
MQXFS COLLAR-PACK ASSEMBLY ITERATIONS

No.	Radial Shim	Pole Key Shim	Pressure Sensitive Film
1	1.575 mm	0	Yes
2	1.524 mm	0	No
3	1.448 mm	0	Yes
4	1.448 mm	0.43mm per side	No
5	1.448 mm	0.46 mm per side	No

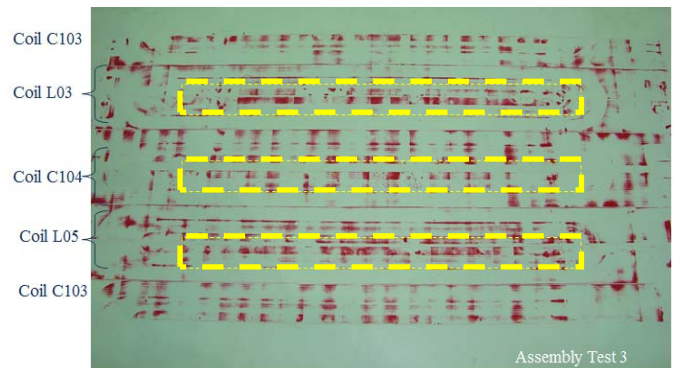


Fig. 4. Print of the pressure sensitive films in the third iteration

A thicker radial shim results in a smaller equivalent inner

diameter (ID) at the collar-coil interface, which causes harder compression on the pole piece than on the coil winding. As seen in LQ [12], it may result in insufficient preload of the pole turn at cold, and thereby causes premature training quenches.

The first three assembly iterations were needed to match this coil-collar interface, and we were able to observe the contact pressure on the coils improving with reduced radial shim thickness. Fig. 4 shows the pressure-sensitive film print obtained after the third assembly iteration. The dark red areas indicate compression observed, which shows the contact pressure beyond the pole areas (highlighted boxes) being distributed more even throughout the coil pack assembly.

The pole keys ensuring the alignment of the coil with respect to the support structure are only located in the coil straight section and must remain clamped by the collars during all the steps of magnet assembly and loading. The keys are nominal in size and need to be azimuthally shimmed after the adjustment of the radial shims to maintain contact between collar and keys. Kapton<sup>®</sup> film is typically used.

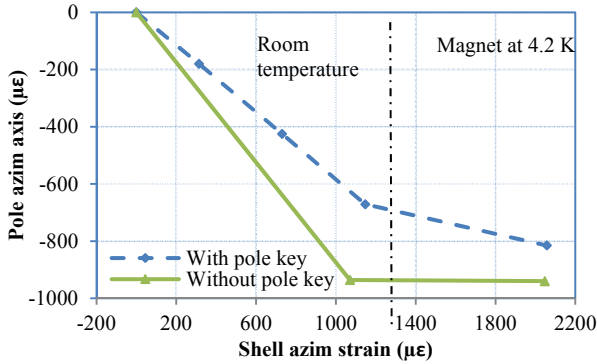


Fig. 5 Comparison of the computed azimuthal strain on the inner layer pole-turn with and without alignment key.

The coil preload regime depends on the contact condition between collar and pole keys. If there is no contact, the entire preload from the shell is transmitted to the coil (without pole key case on Fig. 5). If there is contact between the collar and the key, part of the preload is intercepted by the pole key reducing the coil preload for a given shell strain (with pole key case on Fig. 5). During assembly, in addition to physical measurements of the gap, these transfer functions between shell strain and coil strain are used as a tool to validate the alignment. During the first three assembly builds, a small gap on the order of 40  $\mu\text{m}$  per side between the collars and keys was observed. In the 5<sup>th</sup> assembly iteration, the pole keys were shimmed to a total of 14.6 mm thick to be fully clamped.

#### B. Collar-pack assembly incident and lessons learned

Between two assembly iterations of this short model an incident occurred, causing one of the two top coils to fall to the assembly table. The procedure called for two heavy angle plates to be placed along the length of the collar-pack to support the coils and prevent them from moving outward in both assembling and disassembling processes. Additionally, a

support plug (spud) is inserted into the magnet aperture to support the unrestrained coils during this process. In the second iteration, the spud was not put in position, and coil 104 fell from the assembly when the collar stack was removed. Detailed inspections were taken and all coils were still considered in acceptable condition to be assembled and tested. On the process side, the spud was redesigned to bolt directly to the coils, and improved procedures were implemented, which will also be incorporated in the scale-up of this process to the long model. From a programmatic level, given some uncertainty regarding the coils due to the incident, the upcoming cold test of this magnet is mainly targeting the mechanical performance of MQXFS.

#### C. Coil pack insertion

After the final collar pack assembly, the load pads were assembled around the collars to form the coil pack assembly. Two rolling assembly rails are then attached to the coil pack, and it is inserted into the yoke-shell structure. This assembly process and tooling will be scaled up for the long prototype. Nominal shims in the master key package were calculated from assembly measurements, and these packages are inserted into the structure in preparation for the preload operations.

### IV. ROOM TEMPERATURE PRELOAD

#### A. Preload Target

To avoid coil-to-pole separation under large Lorentz forces, the MQXFS magnet requires precise control of the coil preload in both azimuthal and axial directions. The preload target was calculated with an ANSYS 3D finite element model to ensure the coils remain in compression at the pole during excitation while maintaining the maximum coil stress below 200 MPa after cool-down [13].

Fig. 6 shows the maximum azimuthal stress at 4.2 K inside the coil. By increasing the shimming on the load keys (Fig. 1), the forces from the tensioned shell will be transmitted inwards to the coil. Part of this force is intercepted by the pole/alignment keys. The interception is released after cool-down because of the thermal contraction of the aluminum collars and G11 pole keys, possibly reducing the alignment between coil and structure. Additional studies on pole key material and FEM refinement are needed to ensure complete alignment at cold, and are on-going.

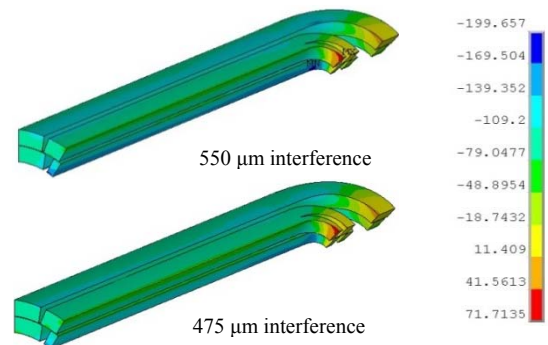


Fig. 6. Azimuthal stress in the coils at cold with different shimming (MPa)

The resulting stress for a 550  $\mu\text{m}$  interference at room temperature reaches the upper limits at cold; therefore, the preload target was chosen conservatively according to the finite element results with an interference of about 475  $\mu\text{m}$ .

The axial load that counteracts the axial Lorentz force on the coils is provided by four pre-tensioned 36 mm diameter aluminum rods and two Nitronic 50 end plates, which prevents the coils from detaching from the pole or end-spacers. Although the rods and plates were sized to accommodate the full axial load,  $F_z$  (see Table I), the magnet was axially preloaded to only  $\sim 40\%$  of this value due to friction forces between the coils and the support structures. This is based on previous experience on the HQ series.

The finite element result of the axial preload system shows total 0.2 MN is generated by the rods at a room temperature with the strain target of 819  $\mu\epsilon$ . This will become 0.58 MN after cool-down.

### B. Preloading and Strain Measurements

Referring to Fig. 1, the bladders are inserted between the iron masters. The gap is opened by the pressurized bladders and then locked in by the shims added to the load keys.

The shells, coils and the aluminum axial rods were instrumented with strain gauges mounted on the four shell mid-planes and on the four coil poles and their stress conditions were monitored and recorded during all room-temperature [9].

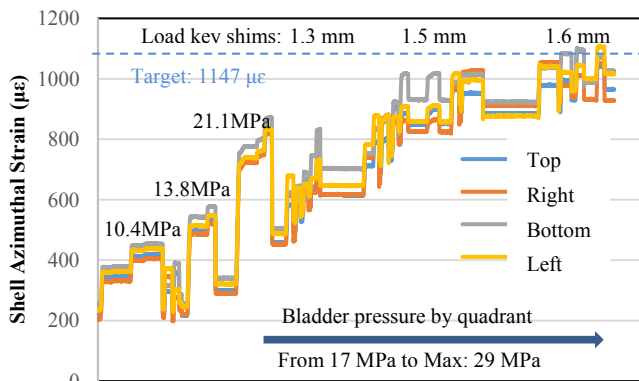


Fig. 7. Strain data of the mid-planes of the shell in the azimuthal pre-loading

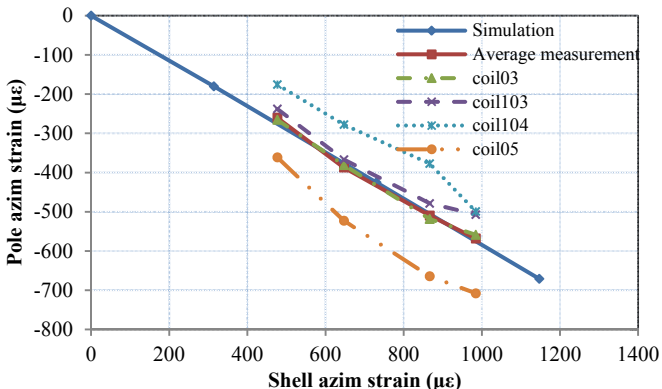


Fig. 8. Comparison of the strain measurements and the finite element simulation

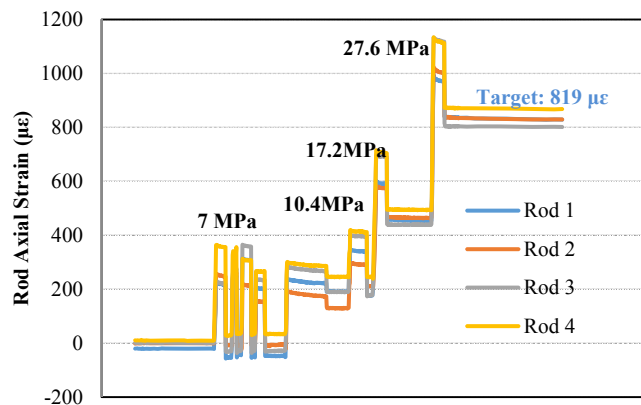


Fig. 9. Axial strain on the rods in the axial pre-loading

Fig. 7 shows the azimuthal strain of 15 degree from the mid-plane of the shell (due to the tack welding slot). The shimming was performed at several steps under different bladder pressures. Initially, all four quadrants were pressurized at the same time. However, at bladder pressures above 24 MPa (3500 psi), the simultaneous shimming of all the coils became difficult; hereby pressurizing the bladders quadrant by quadrant was employed. The maximum pressure reached by the bladders was 28.9 MPa (4200 psi), corresponding to an interference of about 470  $\mu\text{m}$ . The measurements on each location of the shell and the inner layer of the pole piece are plotted in Fig. 8, combined with the predictions of a 3D finite element model. Due to the slight differences on coil size, uneven compression may be applied on each coil and results in the different coil strain. The average strain is used as the indicator of the preload.

The axial loading was applied by a hydraulic cylinder pushing against the endplate. Fig. 9 shows the axial strain on the rods during the loading process. The maximum pressure to reach the target strain was 27.5 MPa (4000 psi), obtained after four steps, at which point the nuts were tightened to lock the tension in the rods.

### CONCLUSION

The MQXFS-AT magnet is the first  $\text{Nb}_3\text{Sn}$  prototype quadrupole using the shell-based structure and incorporating all accelerator grade features to the magnet for alignment and installation in the LHC tunnel. During the magnet assembly, the radial shimming has been studied by cases. The pressure-sensitive paper results indicate that the mechanical alignment between coil and the collar sub-assembly was achieved. The strain data observed during the preload shows agreement with the 3D finite element results, which means the stress inside the coils meets the requirement at both the room temperature and at low temperature. This magnet will be tested in Feb 2015 at FNAL. The assembly experience gained in this assembly will be transferred to the long prototype MQXFA assembly.

### ACKNOWLEDGMENT

The authors would like to thank Thomas Lipton, Ahmet Pekedis and Matthew Reynolds for their dedicated work as well as Shlomo Caspi for the very fruitful discussions.

## REFERENCES

- [1] E. Todesco, *et al.*, “A First Baseline for the Magnets in the High Luminosity LHC Insertion Regions,” *IEEE Trans. Appl. Supercond.*, vol. 24, pp.4003305, June 2014.
- [2] G Ambrosio, H Felice, P Ferracin, “Study of the Minimal Distance Between Two Coils in a Cold-Mass,” *Milestone Report.*, CERN-ACC-2014-0315, 2014.
- [3] M. Juchno, *et al.*, “Mechanical Qualification of the Support Structure for MQXF, the Nb<sub>3</sub>Sn Low- $\beta$  Quadrupole for the High Luminosity LHC,” *IEEE Trans. Appl. Supercond.*, submitted for publication.
- [4] S. Caspi *et al.*, “Design of a 120 mm bore 15 T quadrupole for the LHC upgrade phase II,” *IEEE Trans. Appl. Supercond.*, vol. 20, no. 3, pp. 144–147, Jun. 2010.
- [5] S. Caspi *et al.*, “The Use of Pressurized Bladders for Stress Control of Superconducting Magnets”, *IEEE Trans. On Appl. Supercond.*, Vol. 11, No. 1 , March 2001
- [6] P. Ferracin, “LARP Nb<sub>3</sub>Sn quadrupole magnets for the LHC luminosity upgrade,” in *Proc. AIP Conf.* , vol. 1218, pp. 1291–1300, 2010.
- [7] H. Felice, *et al.*, “Design of HQ—A high field large bore Nb<sub>3</sub>Sn quadrupole magnet for LARP,” *IEEE Trans. Appl. Supercond.*, vol. 19, no. 3, pp. 1235–1238, Jun. 2009.
- [8] P. Ferracin *et al.*, “Mechanical Behavior of HQ01, a Nb<sub>3</sub>Sn Accelerator-Quality Quadrupole Magnet for the LHC Luminosity Upgrade”, *IEEE Trans. On Appl. Supercond.*, Vol. 22, No. 3 , June 2012
- [9] M. Juchno, *et al.*, “Support Structure Design of the Nb<sub>3</sub>Sn Quadrupole for the High Luminosity LHC,” *IEEE Trans. Appl. Supercond.*, vol. 25, no. 3, pp. 1-4, Jun. 2015.
- [10] P. Ferracin, *et al.*, “Assembly and loading of LQS01, a shell-based 3.7 m long Nb<sub>3</sub>Sn quadrupole magnet for LARP,” *IEEE Trans. Appl. Supercond.*, vol. 20, no. 3, pp. 279–282, Jun. 2010.
- [11] G. Ambrosio *et al.*, “Test Results and Analysis of LQS03 Third Long Nb<sub>3</sub>Sn Quadrupole by LARP”, *IEEE Trans. On Appl. Supercond.*, Vol. 23, No 3, June 2013
- [12] G. Ambrosio *et al.*, “Test Results of the First 3.7 m Long Nb<sub>3</sub>Sn Quadrupole by LARP and Future Plans”, *IEEE Trans. On Appl. Supercond.*, Vol. 21, No 3, June 2010
- [13] H. Felice *et al.*, “Test results of TQS03: A LARP shell-based Nb<sub>3</sub>Sn quadrupole using 108/127 conductor”, *9th European Conference on Applied Superconductivity (EUCAS 09)*, Vol. 234, Part 3. 2010.